NANO LETTERS

Letter

Low-Temperature Solution Processing of Graphene#Carbon Nanotube Hybrid Materials for High-Performance Transparent Conductors

Vincent C. Tung, Li-Min Chen, Matthew J. Allen, Jonathan K. Wassei, Kurt Nelson, Richard B. Kaner, and Yang Yang

Nano Lett., **2009**, 9 (5), 1949-1955• Publication Date (Web): 10 April 2009

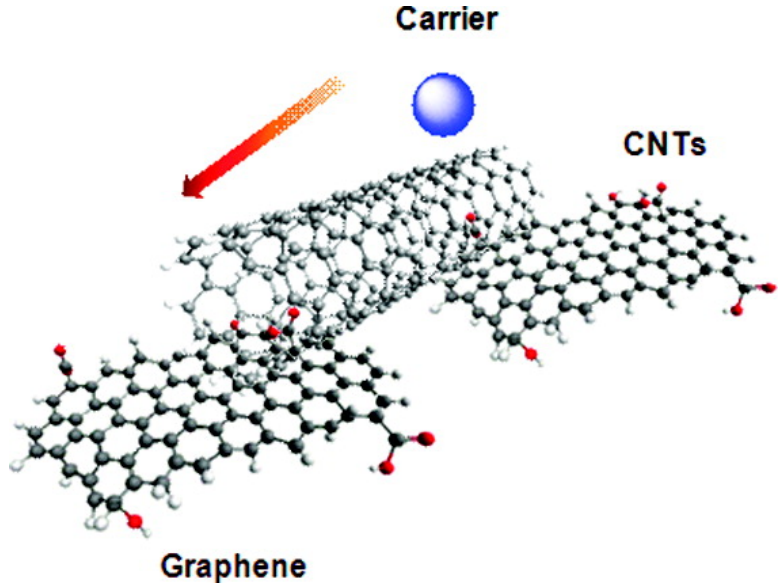

More About This Article

Additional resources and features associated with this article are available within the HTML version:

- Supporting Information
- Access to high resolution figures
- Links to articles and content related to this article
- Copyright permission to reproduce figures and/or text from this article

View the Full Text HTML

Nano Letters is published by the American Chemical Society. 1155 Sixteenth Street N.W., Washington, DC 20036

NANO LETTERS

2009
Vol. 9, No. 5
1949-1955

Low-Temperature Solution Processing of Graphene−Carbon Nanotube Hybrid Materials for High-Performance Transparent Conductors

Vincent C. Tung,[†] Li-Min Chen,[†] Matthew J. Allen,[‡] Jonathan K. Wassei,[‡] Kurt Nelson,[‡] Richard B. Kaner,*[,†,‡] and Yang Yang*[,†]

Department of Materials Science and Engineering and California NanoSystems Institute, University of California, Los Angeles, Los Angeles, California, 90095, and Department of Chemistry and Biochemistry and California NanoSystems Institute, University of California, Los Angeles, Los Angeles, California, 90095

Received January 15, 2009; Revised Manuscript Received March 9, 2009

ABSTRACT

We report the formation of a nanocomposite comprised of chemically converted graphene and carbon nanotubes. Our solution-based method does not require surfactants, thus preserving the intrinsic electronic and mechanical properties of both components, delivering 240 Ω/□ at 86% transmittance. This low-temperature process is completely compatible with flexible substrates and does not require a sophisticated transfer process. We believe that this technology is inexpensive, is massively scalable, and does not suffer from several shortcomings of indium tin oxide. A proof-of-concept application in a polymer solar cell with power conversion efficiency of 0.85% is demonstrated. Preliminary experiments in chemical doping are presented and show that optimization of this material is not limited to improvements in layer morphology.

Since their creation in bulk form in 1991, carbon nanotubes (CNTs) have delivered high axial carrier mobilities in small-scale devices, making them an obvious choice for use as transparent conductors. High aspect ratios lead to low percolation thresholds, meaning very little material is needed for conduction.[1] Thus far, CNTs are capable of delivering resistivities around 500 Ω/□ at 80−85% transmittance.[1−8]

Graphene, a single layer of carbon, has been touted for its potential as an excellent electrical conductor since its experimental discovery in 2004.[9−13] Graphene is essentially a CNT cut along its axis and unrolled to lay flat. It can provide conduction pathways to a greater area per unit mass than CNTs, which should translate into improved conductivity at lower optical densities. The challenge has been in scaling up the mechanical cleavage of graphite.[14] Single-layer samples are most often the result of a laborious peeling method, which is neither scalable nor capable of producing uniform depositions. Recently, researchers have circumvented the problem of mechanical cleavage by using graphite oxide (GO), a layered compound that can be readily dispersed as individual sheets in a good solvent.[15−23] Although GO itself is not electrically conductive, the conjugated network may be restored upon reduction in hydrazine vapor or with high heat after deposition.[18,21,22] However, both reduction methods have their drawbacks, as high temperatures are incompatible with flexible substrates (e.g., poly(ethylene terephthalate), PET) and hydrazine vapors are only able to access and reduce the outer surface of deposited films. Other reduction methods, such as $NaBH_4$, phenyl hydrazine, and KOH in aqueous solution, have been suggested. However, incomplete reduction or large aggregates are often observed. Hence, the resulting graphitic regions are limited, which is detrimental to carrier transport and conductivity. Films of vapor phase reduced GO were reported recently, but displayed a relatively poor conductivity, i.e., 10^4-10^5 Ω/□ at 80% transmittance.[24−29]

Attempts to combine CNTs and chemically converted graphene (CCG) in a single layer have also been reported, but the resulting films were too thick for optical applications.[30,31] By combining CNTs and CCG in a single layer, we envision enhancing the conductivity, while sacrificing little in transparency. As a result, an efficient and facile synthesis to deliver such a hybrid material is of great importance.

To this end, graphite oxide was first synthesized and purified using Hummers method (see Supporting Informa-

* Corresponding authors: Kaner, telephone (310) 825-5346, fax (310) 206-4038; Yang, telephone (310) 825-4052, fax (310) 206-7353.
[†] Department of Materials Science and Engineering and California NanoSystems Institute.
[‡] Department of Chemistry and Biochemistry and California NanoSystems Institute.

10.1021/nl9001525 CCC: $40.75
Published on Web 04/10/2009

Scheme 1

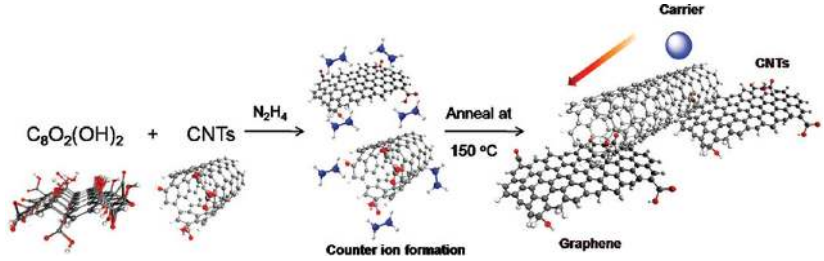

tion). The resulting dry graphite oxide powders were dissolved in deionized (DI) water with the assistance of ultrasonication. The stable dispersion was filtered through an alumina membrane and allowed to dry for several days. Once dried, the graphite oxide paper was carefully peeled from the filter and stored under ambient conditions. In order to enhance the solubility, CNTs were refluxed in a mixture of nitric acid and sulfuric acid to activate the surface with oxygen functionalities. As a result, most of the CNTs are terminated with hydroxyl and carboxylic moieties. After being refluxed for 24 h, the resulting black dispersion was filtered and washed repeatedly with a combination of DI water and ethanol. To produce hybrid suspensions of CCG and CNTs (called G-CNT), dry powders of GO and slightly oxidized CNTs were dispersed directly in anhydrous hydrazine and allowed to stir for 1 day, as shown in Scheme 1.[21] Hydrazine bubbles violently upon contact with the carbon powders but soon forms a uniform dark-gray suspension with no visible solids remaining. A range of compositions were achieved following this protocol, with GO and CNT concentrations observed up to at least 1 mg/mL. A post-treatment process combining ultrasonication and centrifugation can be used to vary the composition of the dispersions before deposition.

To our knowledge this is the first report of dispersing CNTs in anhydrous hydrazine. This is an important observation as it provides a route to deposition that does not involve the use of surfactants, which typically degrade electrical performance. For the stable dispersion of CNTs in hydrazine, we suggest the formation of hydrazinium compounds comprised of negatively charged CNTs surrounded by $N_2H_5^+$ counterions. Such hydrazinium compounds are known to readily disperse in hydrazine.[32] The mechanism for hydrazine reduction of the CNTs is not entirely understood but is

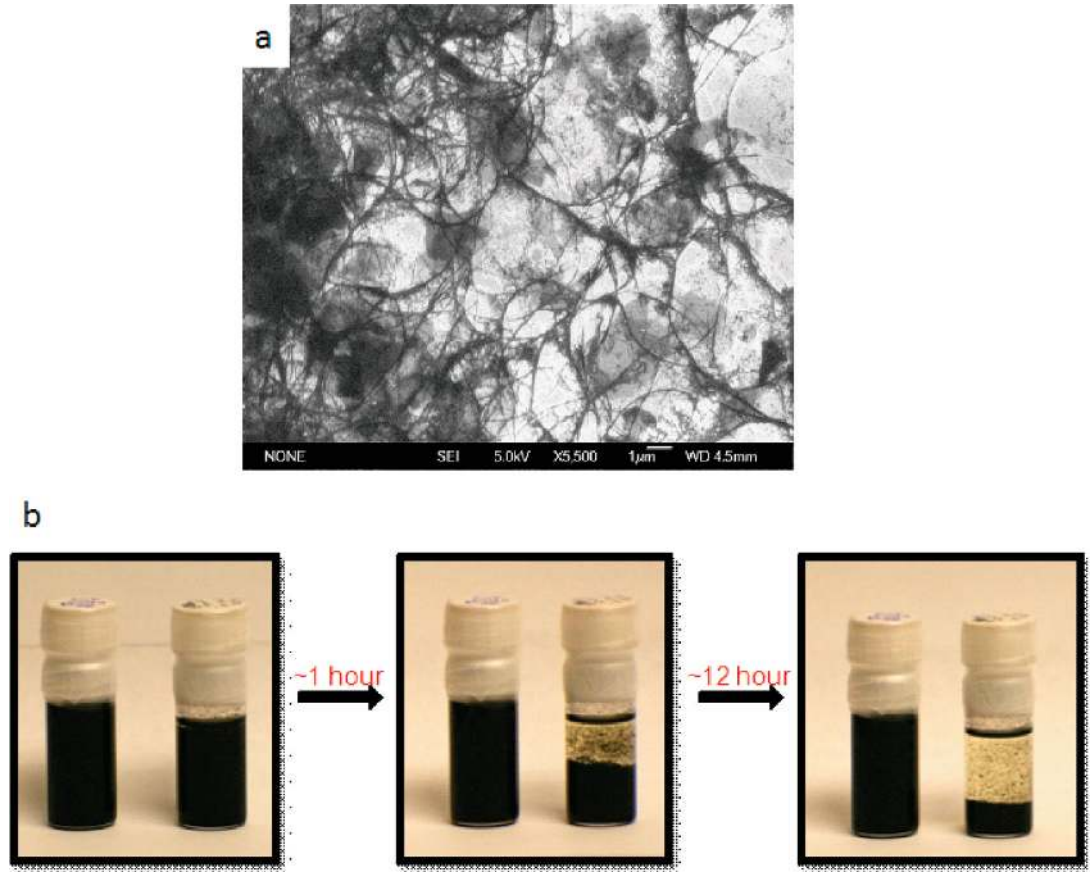

Figure 1. Preparation of chemically converted graphene−SWCNT suspensions. (a) A representative SEM image of a G-CNT film. (b) Photographs of 1 mg of graphite oxide (GO) paper and 5 mg of SWCNT dissolved in pure hydrazine (left) and in dichlorobenzene (DCB) (right), respectively. After 1 h, G-CNT in DCB already precipitates out.

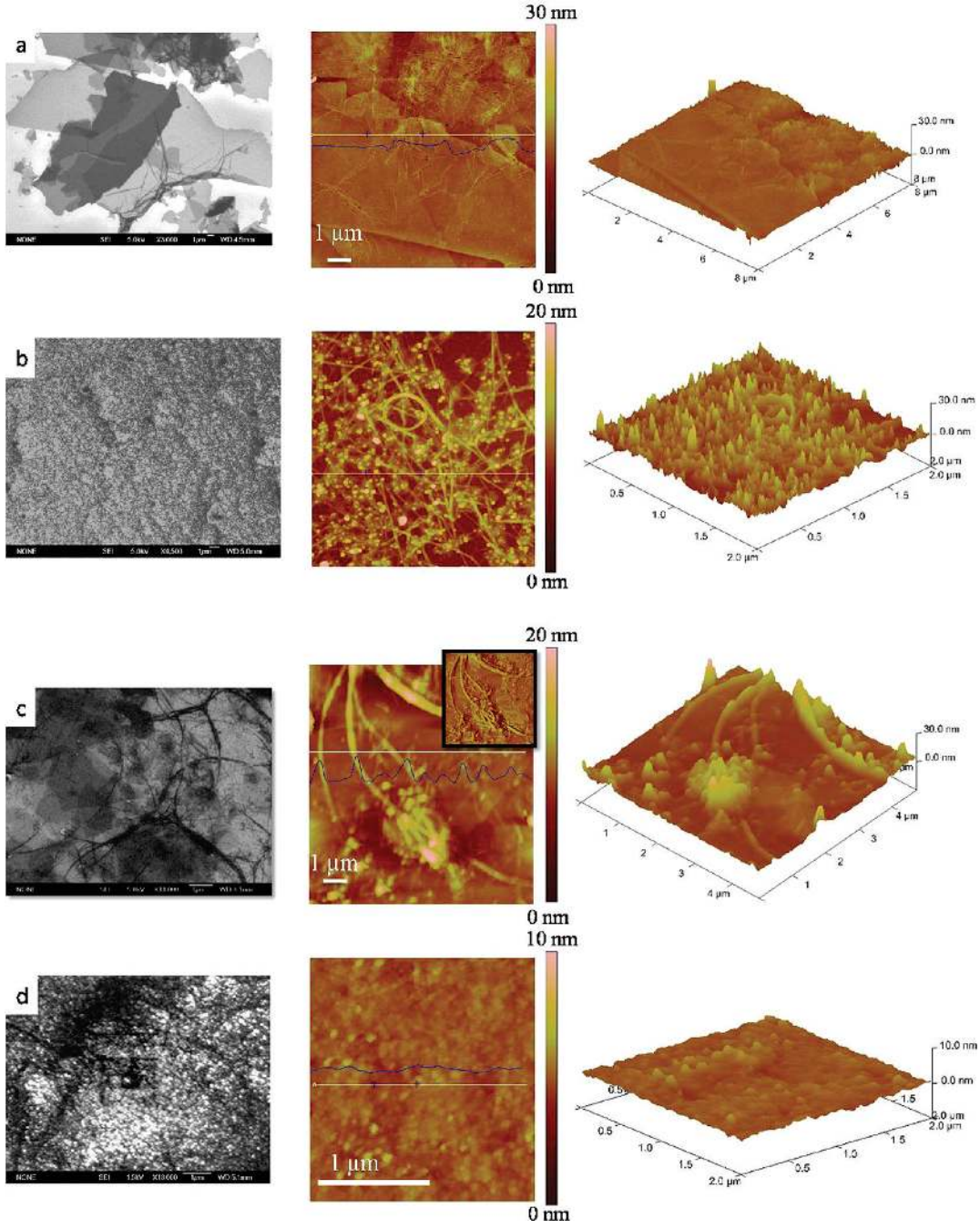

Figure 2. Representative SEM and AFM images of a G-CNT film, along with 3-D topographies of (a) chemically converted graphene, (b) a single-wall carbon nanotube network, and (c) G-CNT hybrid film. Note that the dense network of the G-CNT film exceeds the percolation threshold with average surface roughness of 5−10 nm. Inset: phase image juxtapose the large sheet of chemically converted graphene and individual SWCNT. (d) a G-CNT film after surface optimization. Height profile (blue curve) taken along the white solid line shows an average surface roughness of 1.49 nm.

consistent with our observations of gas evolution upon contact. Unlike CNT suspensions in organic solvents, CNT and G-CNT dispersions in hydrazine are stable for months with little aggregation as shown in Figure 1b. Moreover, UV−vis spectra were carried out to characterize the dispersions (see Supporting Information). Solutions prepared using 1 mg of graphene, 10 mg of CNTs, and a combination of the two were directly dispersed into anhydrous hydrazine. Prior to characterization, ultrasonication was used to ensure a stable dispersion. If one wishes to avoid spin-coating from a solvent of hydrazine's toxicity, the hydrazinium complexes can also be dried and resuspended in DMSO, DMF, and THF before deposition.[21]

G-CNT dispersions were readily deposited onto a variety of substrates by spin-coating and subsequently heated to 150 °C to remove excess solvent. Note that the modest temperature of this post-treatment is fully compatible with flexible substrates, especially in contrast to previously explored procedures used for GO electrodes.[24−29] The present synthesis is facile and provides the following advantages: (i) a one phase reaction without additional surfactants, (ii) the homogeneity and composition of the films is simply determined

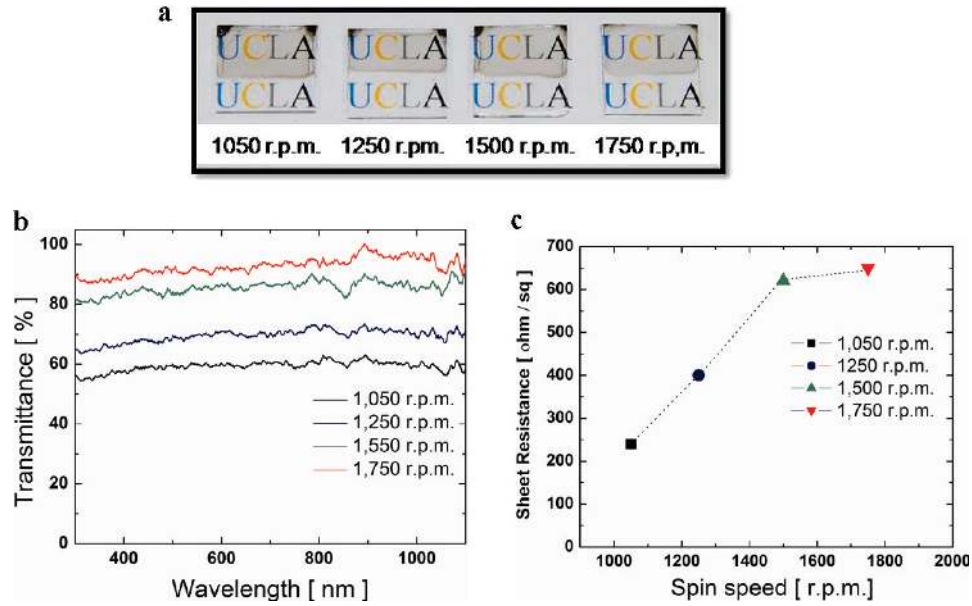

Figure 3. Optical and electrical characterization of G-CNT films. (a) Photographs of G-CNT films with increasing spin speed (from left to right), 1050, 1250, 1500, and 1750 rpm, respectively. (b) Optical transmittance of G-CNT films as a function of different spin speeds. (c) Sheet resistance versus different spin speeds.

by the composition of the parent suspension, spin-coating parameters (speed and duration), and surface modification of the substrate, (iii) relatively inexpensive starting materials, and (iv) high throughput and low temperature processing.

The initial characterization of depositions was carried out by examination with a scanning electron microscope (SEM). Figure 1a provides an SEM image of one such deposited film. These images are used primarily to determine structural information for hybrid films and to understand the effects of different coating conditions. We explored a myriad of spin speeds and durations as well as surface modification of substrates via an O_2 plasma treatment. The image presented shows the percolating network of intertwined graphene and CNTs common to most films. Good contrast in SEM can be difficult to obtain, with relatively low accelerating voltages (1.5−3.0 kV) and probe currents (5−8 μA) delivering the best results on 300 nm Si/SiO_2 substrates.

Although SEM images can be used to understand generally the morphology of the films, they are not accurate representations of topography. Hence, we employed atomic force microscopy (AFM) to establish the thickness and surface roughness of the depositions. Figure 2 shows representative AFM images for single-component films, (a) CNTs and (b) graphene, as well as for the (c) hybrid. The hybrid film is approximately 5 nm thick and exhibits a rough surface covered with CNT bundles/ropes. These bundles are problematic for device fabrication as they often protrude up through the active layers and cause shorting. In order to improve this roughness, G-CNT dispersions were sonicated for 90 min prior to deposition. This treatment was sufficient to break up the CNT bundles and remove the troublesome protrusions, reducing the root mean square surface roughness to ~1.49 nm as shown in Figure 2d.

Once we achieved the desired surface roughness, G-CNT films were deposited on glass substrates and further characterized by UV−vis spectroscopy at normal incidence. Spin speed had the most direct effect on transmittance, as is evident in the photographs and spectra presented in Figure 3. As expected, higher spin speeds delivered thinner films that were more optically transparent, with those deposited at 1050, 1250, 1500, and 1750 rpm displaying optical transmittances of 58%, 70%, 87%, and 92%, respectively. Note that compared with electrodes comprised of graphene only, the addition of CNTs does not appear to significantly increase the overall absorbance. Four-point sheet resistance measurements were made on the same devices after deposition of small gold fingers. Figure 3c shows the relationship between spin speed and sheet resistance. Again the observed relationship is consistent with expectations, with higher spin speeds delivering less material and hence fewer conduction pathways. As shown in the figures, the film deposited at 1750 rpm showed optical transmittance of 92% and a sheet resistance of only 636 Ω/□. Control experiments were also performed on single-component CNTs and graphene films deposited from hydrazine, which reveal sheet resistances of 22 and 490 kΩ/□, respectively (see Supporting Information). Note that the high conductivity of the graphene-only electrode can be attributed to more complete reduction. This sheet resistance is nearly 2 orders of magnitude lower than the analogous vapor reduced GO films reported previously (~1 MΩ/□ and 80−85% transmittance).[13−18] To explain the vast improvement in sheet resistance of a G-CNT electrode, we suggest the formation of an extended conjugated network with individual CNTs bridging the gaps between graphene sheets. The large graphene sheets cover the majority of the total surface area, while the CNTs act as wires connecting the large pads together.

Mechanically, ITO's rigid inorganic crystal structure develops hairline fractures upon bending, which are quite detrimental to the overall electrical performance. To inves-

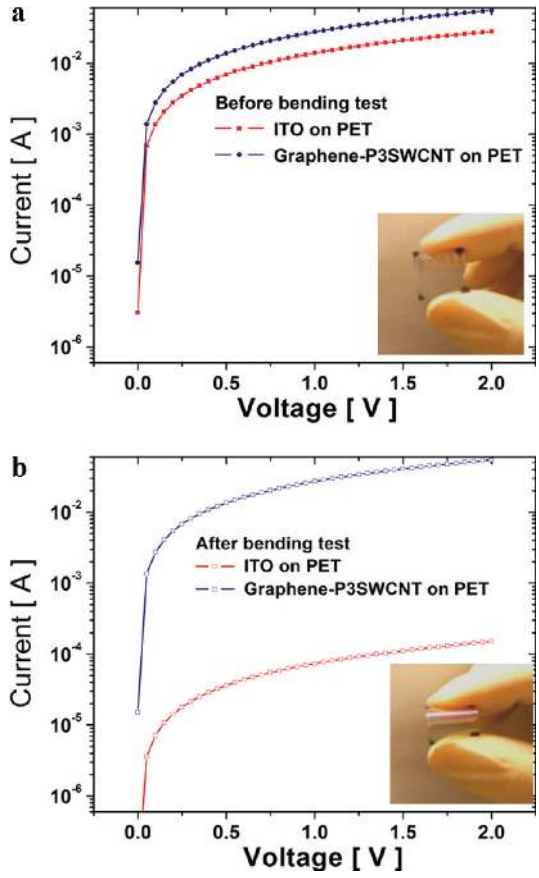

Figure 4. Electrical measurements of G-CNT and ITO films (a) before and (b) after bending at 60° 10 times. The ITO resistance increases 3 orders of magnitude, while the resistance of the G-CNT hybrid electrode remains.

tigate the flexibility of G-CNT electrodes, hydrazine solutions were spin-coated directly on PET substrates. For the densest film, a resistance as low as 44 Ω/□ was observed at 55% transmittance (see Supporting Information). The film's low transmittance is attributed to suboptimal surface morphology.

Parts a and b of Figure 4 present the current−voltage characteristics before and after bending of the G-CNT film and a standard ITO on PET electrode for reference. After bending to 60° more than 10 times, the resistance of the brittle ITO film increased by 3 orders of magnitude, while the G-CNT electrode remained nearly unchanged.

Although G-CNT films perform well during electrical characterization, it is important to understand the feasibility of incorporating this new material in actual optical electronic devices. To this end, we used G-CNT films as a platform for the fabrication of P3HT:PCBM photovoltaic devices. To fabricate the devices, the precleaned glass substrates were subjected to the O_2 plasma to activate the surface. Subsequent to surface treatment, the hydrophilic substrates were brought into contact with PDMS stamps used for patterning the electrode area. Typically, a mixture of 1 mg/mL graphene and 10 mg/mL CNTs were used for spin-coating. The electrodes used were coated on glass and exhibited sheet resistances around 600 Ω/□ at 87% transmittance. The device structure included a thin PEDOT:PSS buffer layer followed by a 2% 1:1 weight ratio of P3HT:PCBM spin-coated and "slow-grown" from dichlorobenzene.[34] Finally, thermal evaporation of Al and Ca provided the reflective cathode.

Similar devices have been reported using vapor reduced GO as the bottom electrode, but high resistivity was detrimental to solar cell performance, i.e., reduced short circuit current (Jsc) and fill factor (FF) resulted in a power conversion efficiency (PCE) of 0.2%.[27,35] The device structure and performance characteristics of our PV devices are presented in Figure 5. With a device area of 4 mm^2, power conversion efficiency (PCE) of 0.85% was measured under illumination of AM 1.5 G. The Jsc, Voc, and FF were 3.47 mA/cm,^{2} 0.583 V, and 42.1%, respectively. The low Jsc and FF are detrimental to PCE and likely due to poor contact at the interface between the G-CNT and the polymer blend. Further engineering of the electrode morphology will likely improve the diode properties of these devices and lead to higher PCEs. That said, the performance of these proof-of-

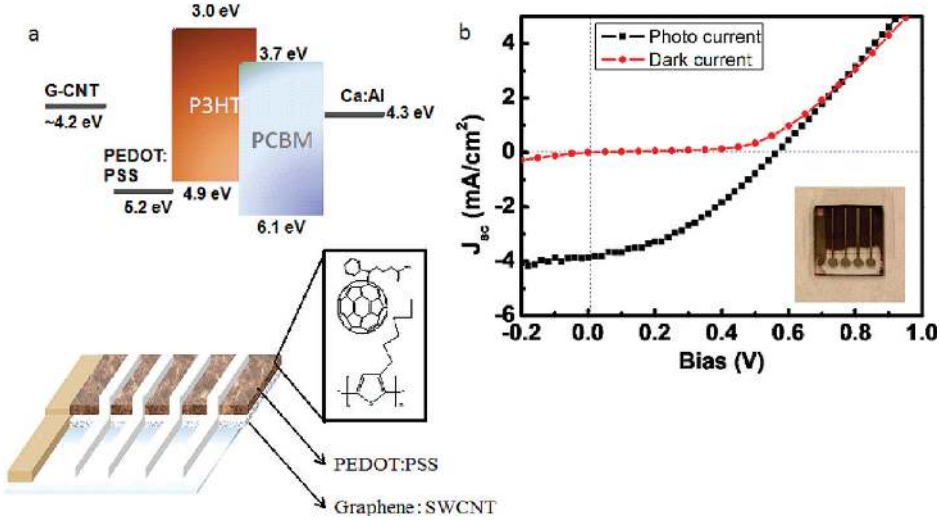

Figure 5. Band diagram, device structure, and current density−voltage (*J*-*V*) curves. (a) The G-CNT based organic solar cell device consists of G-CNT (5 nm)/PEDOT (25 nm)/P3HT:PCBM (230 nm)/Ca: Al (80 nm). (b) Current density voltage (*J*−*V*) curves in the dark (red) and under simulated AM1.5G irradiation (100 mW cm^{-2}) using a xenon-lamp-based solar simulator (black).

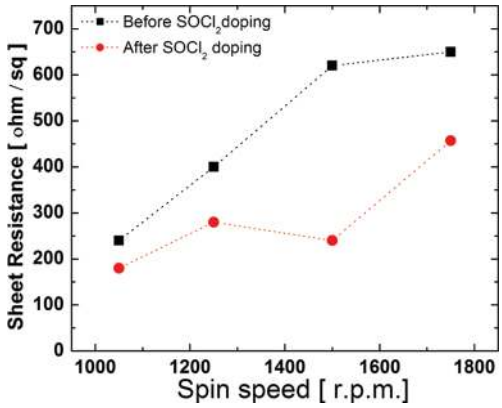

Figure 6. Sheet resistance of G-CNT films before (black) and after (red) chemical doping. An exposure of 15 min to room temperature vapors resulted in a decrease in sheet resistance by a factor of 1.5−2 for all deposited films.

concept devices far exceeds those previously reported and are encouraging for the development of G-CNT electrodes.

Chemical doping has been widely explored as an effective method for increasing the conductivity of CNT electrodes.[7,8,36] Simple treatment with $SOCl_2$ vapor is often employed as a means of anion doping and does not significantly affect the optical transmittance of CNT films. We used a similar method for this hybrid system by exposing as-deposited G-CNT films to $SOCl_2$ vapors after spin-coating. The sheet resistance before and after treatment is recorded in Figure 6. An exposure of 15 min to room temperature $SOCl_2$ vapors resulted in a decrease in sheet resistance by a factor of 1.5−2 for all deposited films. The sheet resistance for the 1500 rpm film was reduced from 636 to 240 Ω/□ after doping, while transmittance dropped only slightly from 88 to 86%. To confirm the mechanism of anion doping, similar experiments were performed using I_2 vapors and delivered comparable results. These initial doping experiments indicate that further improvements are likely.

Here we report a competitive synthetic approach using a hybrid layer of carbon nanotubes and chemically converted graphene. This technology is facile, inexpensive, scalable, and compatible with flexible substrates. We present conductivity and optical data demonstrating comparable performance to the ITO used in flexible applications, 240 Ω/□ at 86% transmittance after chemical doping, and also a proof-of-concept application in a polymer solar cell with a power conversion efficiency (PCE) of 0.85%. Our preliminary experiments using chemical doping show that optimization of this material is not limited to improvements in layer morphology. With future work, this versatile material could well provide an appropriate transparent electrode for tomorrow's optical electronics.

Acknowledgment. This work has been partially supported by National Science Foundation Grant DMR-0507294, its NSF-IGERT program (M.J.A. and L.-M.C.), and the Air Force Office of Scientific Research Grant FA95500710264 (Y.Y.). The authors would also like to thank Scott Gilje and Sergey Dubin for their help in synthesizing graphite oxide and Kate Chuang for the computer graphic design.

Supporting Information Available: Descriptions of graphite oxide synthesis, purification of G-CNT electrodes, chemical doping of G-CNT electrodes, and UV, XPS, and UPS analysis, figures of UV-vis spectra of graphene, representative SEMs and AFMs, XPS analysis, UPS spectrum of a G-CNT film, and representative images of G-CNT, and a table of transmittance and sheet resistance of selected thin films. This material is available free of charge via the Internet at http://pubs.acs.org.

References

(1) Hu, L.; Hecht, D. S.; Gruner, G. *Nano Lett.* **2004**, *4*, 2513.
(2) Wu, Z. C.; Chen, Z. H.; Du, X.; Logan, J. M.; Sippel, J.; Nikolou, M.; Kamaras, K.; Reynolds, J. R.; Tanner, D. B.; Hebard, A. F.; Rinzler, A. G. *Science* **2004**, *305*, 1273.
(3) Hu, L. B.; Gruner, G.; Li, D.; Kaner, R. B.; Cech, J. *J. Appl. Phys.* **2007**, *101*, 016102.
(4) Li, J.; Hu, L.; Wang, L.; Zhou, Y.; Gruner, G.; Marks, T. J. *Nano Lett.* **2006**, *6*, 2472.
(5) Zhang Zhang, D. H.; Ryu, K.; Liu, X. L.; Polikarpov, E.; Ly, J.; Tompson, M. E.; Zhou, C. W. *Nano Lett.* **2006**, *6*, 1880.
(6) Ago, H.; Petritsch, K.; Shaffer, M. S. P.; Windle, A. H.; Friend, R. H. *Adv. Mater.* **1999**, *11*, 1281.
(7) Rowell, M. W.; Topinka, M. A.; McGehee, M. D.; Prall, H. J.; Dennler, G.; Sariciftci, N. S.; Hu, L. B.; Gruner, G. *Appl. Phys. Lett.* **2006**, *88*, 233506.
(8) Pasquier, A. D.; Unalan, H. E.; Kanwal, A.; Miller, S.; Chhowalla, M. *Appl. Phys. Lett.* **2005**, *87*, 203511.
(9) Novoselov, K. S.; Geim, A. K.; Morozov, S. V.; Jiang, D.; Zhang, Y.; Dubonos, S. V.; Grigorieva, I. V.; Firsov, A. A. *Science* **2004**, *306*, 666.
(10) Gusynin, V. P.; Sharapov, S. G. *Phys. Rev. Lett.* **2005**, *95*, 146801.
(11) Zhang, Y. B.; Tan, Y. W.; Stormer, H. L.; Kim, P. *Nature (London)* **2005**, *438*, 201.
(12) Novoselov, K. S.; McCann, E.; Morozov, S. V.; Fal'ko, V. I.; Katsnelson, M. I.; Zeitler, U.; Jiang, D.; Schedin, F.; Geim, A. K. *Nat. Phys.* **2006**, *2*, 177.
(13) Novoselov, K. S.; Jiang, Z.; Zhang, Y.; Morozov, S. V.; Stormer, H. L.; Zeitler, U.; Maan, J. C.; Boebinger, G. S.; Kim, P.; Geim, A. K. *Science* **2007**, *315*, 1379.
(14) Watcharotone, S.; Dikin, D. A.; Stankovich, S.; Piner, R.; Jung, I.; Dommett, G. H. B.; Evmenenko, G.; Wu, S. E.; Chen, S. F.; Liu, C. P.; Nguyen, S. T.; Ruoff, R. S. *Nano Lett.* **2007**, *7*, 1888.
(15) Jung, I.; Pelton, M.; Piner, R.; Dikin, D. A.; Stankovich, S.; Watcharotone, S.; Hausner, M.; Ruoff, R. S. *Nano Lett.* **2007**, *7*, 3569.
(16) Stankovich, S.; Piner, R. D.; Nguyen, S. T.; Ruoff, R. S. *Carbon* **2006**, *44*, 3342.
(17) Hummers, W. S.; Offeman, R. E. *J. Am. Chem. Soc.* **1958**, *80*, 1339.
(18) Gilje, S.; Han, S.; Wang, M.; Wang, K. L.; Kaner, R. B. *Nano Lett.* **2007**, *7*, 3394.
(19) Gomez-Navarro, C.; Weitz, R. T.; Bittner, A. M.; Scolari, M.; Mews, A.; Burghard, M.; Kern, K. *Nano Lett.* **2007**, *7*, 3499.
(20) Li, X. L.; Wang, X. R.; Zhang, L.; Lee, S. W.; Dai, H. J. *Science* **2008**, *319*, 1229.
(21) Tung, V. C.; Allen, M. J.; Yang, Y.; Kaner, R. B. *Nat. Nanotechnol.* **2009**, *4*, 25.
(22) Li, D.; Mueller, M. B.; Gilje, S.; Kaner, R. B.; Wallace, G. G. *Nat. Nanotechnol.* **2008**, *3*, 101.
(23) Hernandez, Y.; Nicolosi, V.; Lotya, M.; Blighe, F. M.; Sun, Z. Y.; De, S.; McGovern, I. T.; Holland, B.; Byrne, M.; Gun'ko, Y. K.; Boland, J. J.; Niraj, P.; Duesberg, G.; Krishnamurthy, S.; Goodhue, R.; Hutchison, J.; Scardaci, V.; Ferrari, A. C.; Coleman, J. N. *Nat. Nanotechnol.* **2008**, *3*, 563.
(24) Li, X. L.; Zhang, G. Y.; Bai, X. D.; Sun, X. M.; Wang, X. R.; Wang, E.; Dai, H. J. *Nat. Nanotechnol.* **2008**, *3*, 538.
(25) Wang, X.; Zhi, L. J.; Mullen, K. *Nano Lett.* **2008**, *8*, 323.
(26) Wang, X.; Zhi, L. J.; Tsao, N.; Tomovic, Z.; Li, J. L.; Mullen, K. *Angew. Chem., Int. Ed.* **2008**, *47*, 2990.
(27) Eda, G.; Fanchini, G.; Chhowalla, M. *Nat. Nanotechnol.* **2008**, *3*, 270.
(28) Becerril, H. A.; Mao, J.; Liu, Z.; Stoltenberg, R. M.; Bao, Z.; Chen, Y. *ACS Nano* **2008**, *2*, 463.
(29) Wu, J. B.; Becerril, H. A.; Bao, Z. N.; Liu, Z. F.; Chen, Y. S.; Peumans, P. *Appl. Phys. Lett.* **2008**, *92*, 263302.
(30) Cai, D. Y.; Song, M.; Xu, C. X. *Adv. Mater.* **2008**, *20*, 1706.

(31) Yu, A. P.; Ramesh, P.; Sun, X. B.; Bekyarova, E.; Itkis, M. E.; Haddon, R. C. *Adv. Mater.* **2008**, *20*, 4740.
(32) Mitzi, D. B.; Copel, M.; Chey, S. J. *Adv. Mater.* **2005**, *17*, 1285.
(33) Holzinger, M.; Abraha, J.; Whelan, P.; Graupner, R.; Ley, L.; Hennrich, F.; Kappes, M.; Hirsch, A. *J. Am. Chem. Soc.* **2003**, *125*, 8566.
(34) Li, G.; Shrotriya, V.; Huang, J. S.; Yao, Y.; Moriarty, T.; Emery, K.; Yang, Y. *Nat. Mater.* **2005**, *4*, 864.
(35) Eda, G.; Lin, Y. Y.; Miller, S.; Chen, C. W.; Su, W. F.; Chhowalla, M. *Appl. Phys. Lett.* **2008**, *92*, 233305.
(36) Dettlaff-Weglikowska, U.; Skakalova, V.; Graupner, R.; Jhang, S. H.; Kim, B. H.; Lee, H. J.; Ley, L.; Park, Y. W.; Berber, S.; Tomanek, D.; Roth, S. *J. Am. Chem. Soc.* **2005**, *127*, 5125.

NL9001525